This article is made available via the ACS COVID-19 subset for unrestricted RESEARCH re-use and analyses in any form or by any means with acknowledgement of the original source. These permissions are granted for the duration of the World Health Organization (WHO) declaration of COVID-19 as a global pandemic.

ACS Medicinal Chemistry Letters

pubs.acs.org/acsmedchemlett

Note

TMPRSS2 Inhibitor Discovery Facilitated through an *In Silico* and Biochemical Screening Platform

Amanda L. Peiffer,[¶] Julie M. Garlick,[¶] Yujin Wu, Jesse W. Wotring, Sahil Arora, Alexander S. Harmata, Daniel A. Bochar, Corey J. Stephenson, Matthew B. Soellner, Jonathan Z. Sexton, Charles L. Brooks, III,* and Anna K. Mapp*

Cite This: *ACS Med. Chem. Lett.* 2023, 14, 860−866

Read Online

ACCESS | Metrics & More | Article Recommendations | Supporting Information

ABSTRACT: The COVID-19 pandemic has highlighted the need for new antiviral approaches because many of the currently approved drugs have proven ineffective against mitigating SARS-CoV-2 infections. The host transmembrane serine protease TMPRSS2 is a promising antiviral target because it plays a role in priming the spike protein before viral entry occurs for the most virulent variants. Further, TMPRSS2 has no established physiological role, thereby increasing its attractiveness as a target for antiviral agents. Here, we utilize virtual screening to curate large libraries into a focused collection of potential inhibitors. Optimization of a recombinant expression and purification protocol for the TMPRSS2 peptidase domain facilitates subsequent biochemical screening and characterization of selected compounds from the curated collection in a kinetic assay. In doing so, we identify new noncovalent TMPRSS2 inhibitors that block SARS-CoV-2 infectivity in a cellular model. One such inhibitor, debrisoquine, has high ligand efficiency, and an initial structure−activity relationship study demonstrates that debrisoquine is a tractable hit compound for TMPRSS2.

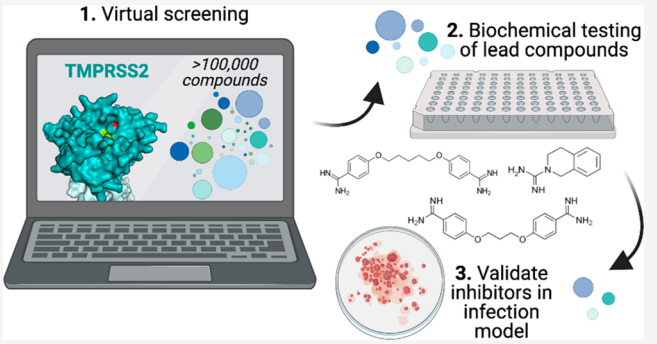

KEYWORDS: *in silico screening, TMPRSS2, antiviral therapeutics, fragment inhibitor, reversible inhibitor*

The emergence of COVID-19 in late 2019 and the ongoing global impact has prompted an urgent need for effective treatments.[1] As with many coronoviruses, infection with nearly all SARS-CoV-2 variants requires host cell cooperation; the spike (S) protein protruding outside the viral coat requires priming by TMPRSS2, a human transmembrane serine protease, for viral entry via the receptor angiotensin-converting enzyme 2 (ACE2) (Figure 1A).[2,3] The biological function of TMPRSS2 is largely unknown, with data suggesting it is likely functionally redundant.[4,5] Along with SARS-CoV-2, TMPRSS2 has been implicated in priming other pathogenic coronaviruses, such as SARS-CoV and MERS, as well as influenza.[6−10] TMPRSS2$^{-/-}$ mice exhibited limited phenotypic differences compared with wild-type animals, yet the knockout conferred resistance to viral infections.[11] Inhibiting the expression of TMPRSS2 via bromodomain and extra-terminal (BET) motif inhibitors leads to decreased infectivity of SARS-CoV-2 in human lung cells, thereby further suggesting the viability of TMPRSS2 inhibition as an antiviral strategy.[12] Thus, TMPRSS2 is a desirable drug target for many viral infections.

The search for TMPRSS2 inhibitors has been challenging, although recent studies have identified ketobenzothiazole-based peptide[13] and peptidomimetic[14] inhibitors.[15] Recent *in silico* studies identified noncovalent architectures that have good biochemical inhibition of TMPRSS2 but little to no activity in cell assays.[16] Camostat, a compound initially discovered as a matriptase-2 inhibitor, also inhibits TMPRSS2, along with nafamostat and gabexate.[2,17] Both camostat and nafamostat inhibit a wide range of serine proteases and are rapidly metabolized in mammals to structures with poorly defined activity.[18−23] Small molecule TMPRSS2 inhibitors with less reactive architectures that are structurally amenable for optimization are therefore desired.

Here, we report the development of a combined *in silico* and biochemical workflow to identify and validate new small molecule TMPRSS2 inhibitors. Our protocol for virtual screening against a TMPRSS2 homology model comprised a molecular dynamics/simulated annealing-based docking that employed flexible receptor side chains to capture subtle changes, both conformational and energetic, for much

Received: January 27, 2023
Accepted: May 18, 2023
Published: May 30, 2023



ACS Publications

© 2023 American Chemical Society

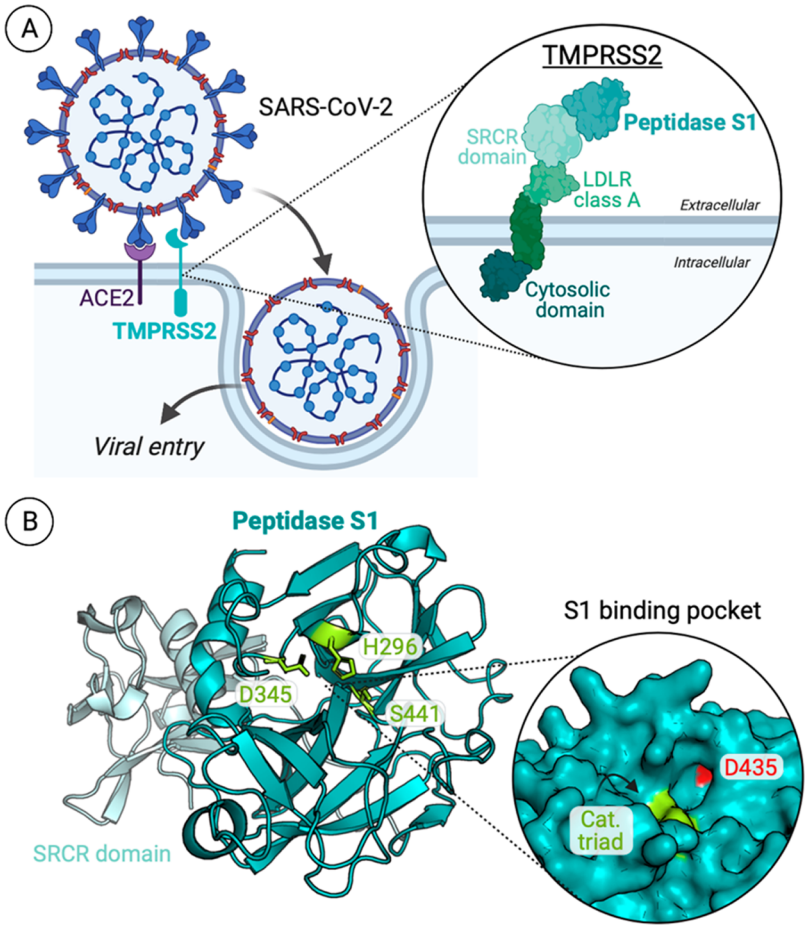

Figure 1. Role of TMPRSS2 in SARS-CoV-2 infection. (A) TMPRSS2 primes the viral S protein (SARS-2-S), which promotes membrane fusion and ultimately viral entry.[2] The extracellular portion of the protein is composed of a LDLR class A domain, an SRCR domain, and the peptidase S1 domain required for catalytic activity.[24] (B) The peptidase S1 domain of TMPRSS2 cleaves SARS-2-S at the S2′ cleavage site.[25,26]

improved compound scoring. This approach curated a subset of potential TMPRSS2 ligands, which upon subsequent biochemical testing were identified as active inhibitors. The compounds identified were active in cell-based viral entry assays, and this activity was shown to be dependent on TMPRSS2. An initial structure−activity relationship study of one of the hits, debrisoquine, further demonstrated that analogues of this compound could serve as potent TMPRSS2 inhibitors.

Virtual screening methods have greatly improved over the past two decades, which has led to many drug discovery campaigns by filtering out thousands/millions of molecules before testing them *in vitro*. Because no crystallographic or NMR-based models existed for TMPRSS2 at the time of this work, we developed a homology model for the active soluble domain starting from prediction using the SWISS-MODEL web interface (Figure S8).[27] Comparing our homology model to the reported crystallographic structure of TMPRSS2 that was solved after our studies,[28] we find that the predicted structure overlays well with the peptidase domain (Figure S8).

Extensive virtual screening was performed to obtain putative hits for follow-up testing via *in vitro* inhibition assays. A total of 134 109 molecules was collected from multiple databases, which were subjected to a hierarchical refinement of docking poses. In the first stage, rigid receptor docking was performed by exploring two means of initially positioning the small molecules. One utilized a novel 3D pharmacophore *fastdock* framework, which operates by superposing pharmacophores onto compounds bound in experimentally solved structures in other bound serine protease structures; the other initiated from a random generation of molecular conformations and random positioning inside the pocket (Figure 2A). From this initial stage, 4307 Level 1 screening candidates were determined and subjected to GPU-accelerated Flexible-CDOCKER methods that were recently developed as part of the CHARMM molecular modeling package.[29−31] This approach utilizes flexible side chains for residues in or near the binding pocket while using a grid representation for the remaining receptor.

The virtual screen was successful on many fronts. MD-based flexible docking identified residues near the active site that are conformationally dynamic to accommodate different ligands. Residues Gln-438 and Lys-342 show the greatest conformational change upon ligand binding, thereby suggesting that they participate in stabilizing bound compounds. Known inhibitors camostat, nafamostat, and gabexate ranked in the top five compounds and adopted poses that demonstrate how the catalytic serine residue positions itself to ultimately react with the inhibitors while positioning the guanidinium functionality to form a salt bridge interaction with the active site Asp-435; this is consistent with our biochemical assay data, which indicates that these inhibitors function through covalent bond formation (Figures S5 and S6). As the mechanism of covalent inhibition likely involves His-296 deprotonating Ser-441, we performed a subsequent docking experiment using the three

https://doi.org/10.1021/acsmedchemlett.3c00035
ACS Med. Chem. Lett. 2023, 14, 860−866

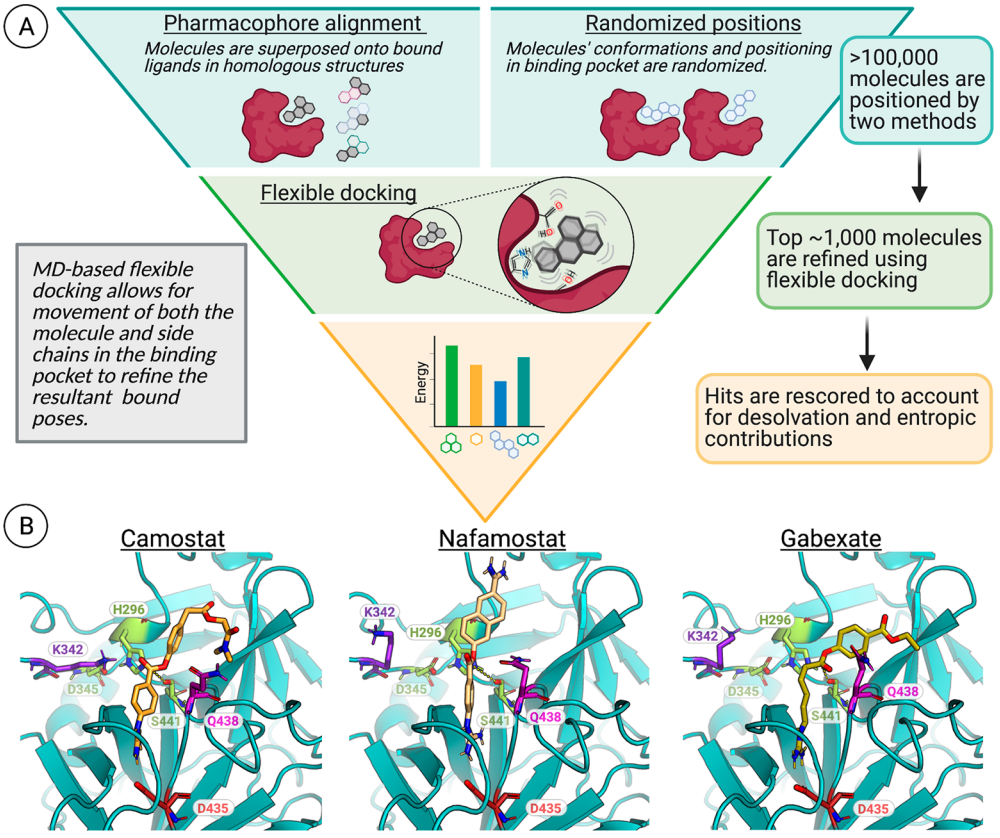

Figure 2. (A) The virtual screening protocol involves multiple refinements, including using MD-based docking. (B) Docked poses of camostat, nafamostat, and gabexate in the TMPRSS2 active site with the proton transfer from Ser-441 to His-296 that occurs after substrate binding. Shown in red is D435, which resides at the bottom of the S1 binding pocket, and lime green corresponds to the catalytic triad (His-296, Asp-345, Ser-441). Dashed lines shown here indicate the distance between the catalytic serine oxygen and the carbonyl carbon of each inhibitor (camostat = 3.5 Å, nafamostat = 4.8 Å, gabexate = 3.5 Å).

molecules with these charge changes (Figure 2B). For all three molecules, the deprotonated serine moved closer to the carbonyl carbon of the inhibitor. In the case of camostat, for example, the distance decreased from 4.9 to 3.5 Å, and the angle changed from 143° to 127°, which is consistent with eventual nucleophilic attack.[32−34] Additionally, this is consistent with the crystal structure of a nafamostat-bound structure of TMPRSS2.[28]

Several clinically approved drugs emerged as top 20 compounds in the virtual screen, which we selected to test in an *in vitro* screening assay. The format of the assay was based on conditions previously reported, with the exception that an optimized expression and refolding protocol for the TMPRSS2 peptidase domain [TMPRSS2(247−492)] was developed [see the Supporting Information (SI) for details].[18,35] Like the covalent inhibitors, pentamidine, propamidine, and debrisoquine all contain a guanidinium moiety and docked into the active site of TMPRSS2 with the positive charge pointing toward Asp-435 (Figure 3A). Biochemically, we found that all three molecules did inhibit TMPRSS2 (Figure 3B). The docked poses of pentamidine and propamidine show both compounds are positioned to block the active site residues, whereas debrisoquine does not fully span the catalytic triad, which likely contributes to the differences in potency (Figure 3A,B). Pentamidine and propamidine are of similar size to camostat and nafamostat, which is typical of small molecule inhibitors (>350 mol wt), while debrisoquine is quite small at 175.2 mol wt, which classifies it as a fragment. Debrisoquine has the greatest ligand efficiency (LE) at 0.42 (kcal/mol)/heavy atom compared with pentamidine and propamidine, which are 0.33 and 0.31 (kcal/mol)/heavy atom, respectively.

Debrisoquine, pentamidine and propamidine were tested for their ability to inhibit SARS-CoV-2 viral infection in Calu-3 cells, a human lung cell line (Figure 3C), and camostat was included as a control (Figure S9). Of the three molecules discovered from our screening process, debrisoquine showed the greatest inhibition of viral infection, with an IC_{50} value of 22 ± 1 μM and no decrease in cell viability up to 500 μM (Figure 3D). Validation of TMPRSS2-dependent inhibition was tested in viral infectivity assays using the human intestinal epithelial cell line Caco-2. Caco-2 cells express significantly lower levels of TMPRSS2 than do Calu-3 cells.[36] Further, SARS-CoV-2 viral entry in Caco-2 cells has been shown to be far less dependent on TMPRSS2, with entry occurring via a cathepsin-mediated mechanism.[37] We found that debrisoquine was unable to inhibit infection of Caco-2, thereby confirming the TMPRSS2-specific mechanism of action for debrisoquine (Figure S10). Thus, the high ligand efficiency in our *in vitro* assays in conjunction with the reduced viral infection seen in the Calu-3 cellular model suggests that debrisoquine would be an excellent starting point for fragment expansion to increase potency for TMPRSS2 inhibition.

The flexible docking results with debrisoquine suggested that the fragment could be elongated through 6-benzamido substitutions to better occupy the binding pocket in

https://doi.org/10.1021/acsmedchemlett.3c00035
ACS Med. Chem. Lett. 2023, 14, 860−866

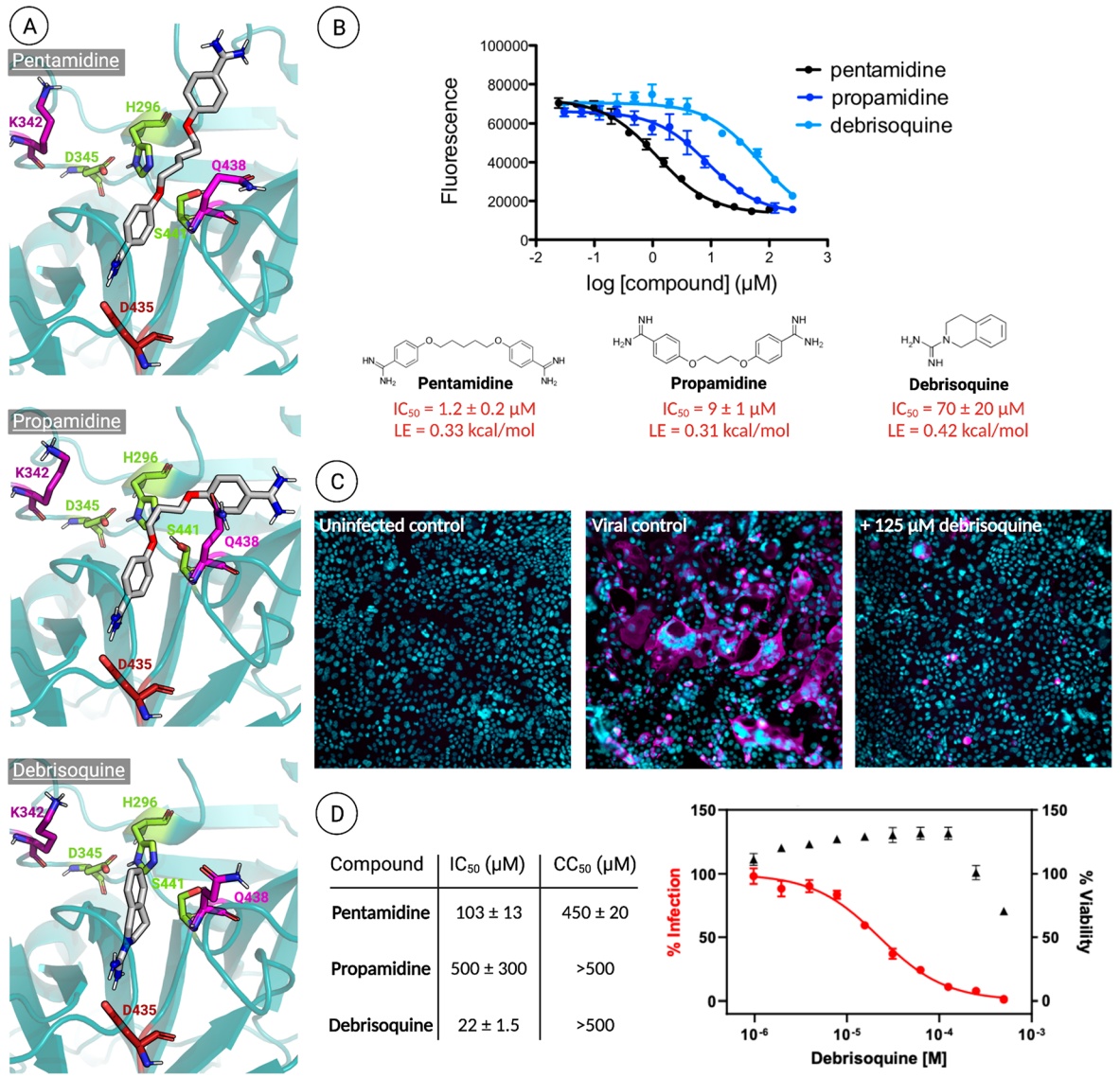

Figure 3. (A) Docking results for the three drugs identified as hits both in the virtual screen and the *in vitro* assay. All three molecules fit into the active site (Asp-435 at the bottom of the pocket shown in red). Pentamidine and propamidine obstruct access to the catalytic triad (residues shown in lime green), whereas the fragment debrisoquine only partially reaches those residues. (B) Computational hits inhibit TMPRSS2 in biochemical activity assay. Top: inhibition assays to obtain IC_{50} curves. Data is the average of duplicate experiments conducted in technical triplicate. Calculated IC_{50} values and ligand efficiencies (LE) are shown below the chemical structures of the hits. (C) TMPRSS2 inhibitors have *in vitro* efficacy in the human lung cell line Calu-3. Representative images (10× magnification) of viral and uninfected controls for the anti-SARS-CoV-2 bioassay. Nuclei are shown in cyan, and viral nucleocapsid protein is shown in magenta. Right: representative image for the most efficacious (nontoxic) concentrations of debrisoquine. (D) Left: IC_{50} and cytotoxic concentration (CC_{50}; concentration of compound that reduces viable cells by 50% as compared to a control) values for the three inhibitors calculated from the infectivity assay. Camostat activity was 1 μM (IC_{50}) and >500 mM (CC_{50}), with details in SI Figure S9. Right: the inhibition curve from the infectivity assay for debrisoquine.

TMRPSS2. Thus, a small library of 6-benzamido-substituted debrisoquine analogues (**7a**–**h**) were synthesized to assess the tractability of debrisoquine as a TMPRSS2 inhibitor scaffold (Figure 4; see the Supporting Information for full details). The resulting analogues were compared with debrisoquine in a kinetic biochemical assay using the Boc-QAR-AMC substrate and TMRPSS2(106–492). Under these conditions, the parent debrisoquine had an IC_{50} of 23 ± 11 μM, which is in line with the EC_{50} values in the cellular experiments. Several analogues exhibited significantly improved activity against TMPRSS2. For example, **7c** had an IC_{50} = 4 ± 1 μM, and the naphthyl analogues had similarly potent IC_{50} values (**7d**, IC_{50} = 3.4 ± 0.8 μM; **7h**, IC_{50} = 4 ± 2 μM). Thus, debrisoquine is a tractable starting point for the development of more potent and reversible TMPRSS2 inhibitors.

With new strains of SARS-CoV-2 emerging and the contribution of TMPRSS2 to infectivity of multiple coronaviruses, it is critical that effective strategies to inhibit TMPRSS2 protease activity are developed.[38,39] However, TMPRSS2 provides obstacles in multiple areas of the discovery pipeline. In the present study, we demonstrate that our combined computational and experimental strategy can be used to identify new TMPRSS2 protease inhibitors. Computational screening provides initial triage through large compound libraries, which allows a smaller number of molecules, more likely to be functionally relevant, to be tested in a biochemical

https://doi.org/10.1021/acsmedchemlett.3c00035
ACS Med. Chem. Lett. 2023, 14, 860–866

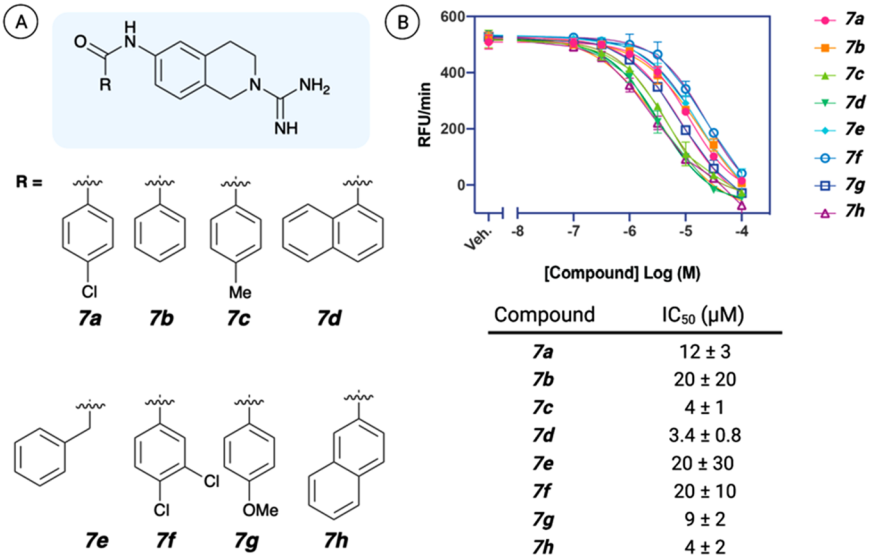

Compound	IC_{50} (μM)
7a	12 ± 3
7b	20 ± 20
7c	4 ± 1
7d	3.4 ± 0.8
7e	20 ± 30
7f	20 ± 10
7g	9 ± 2
7h	4 ± 2

Figure 4. (A) Structures of debrisoquine analogues. Full characterization data and additional experimental details are provided in the SI. (b) The analogues were tested in a kinetic assay with TMPRSS2(106−492) and the Boc-QAR-AMC substrate. IC_{50} values were calculated from the data obtained from three independent experiments with the indicated error (SD).

assay. This is particularly relevant in the context of proteins such as TMPRSS2 that provide a challenge to express actively in high yields. We identified debrisoquine as a TMPRSS2 inhibitor that is active in cell-based viral entry assays in a TMPRSS2-depedent manner. A small panel of debrisoquine analogues demonstrated that rapid improvement of TMPRSS2 inhibitory activity can be obtained and that this scaffold remains promising for further elaboration.

■ ASSOCIATED CONTENT

Supporting Information

The Supporting Information is available free of charge at https://pubs.acs.org/doi/10.1021/acsmedchemlett.3c00035.

Full biochemical, computational, and synthetic methods and full characterization data of all new compounds with supplemental figures (PDF)

■ AUTHOR INFORMATION

Corresponding Authors

Charles L. Brooks, III − *Program in Chemical Biology, Department of Chemistry, and Department of Biophysics, University of Michigan, Ann Arbor, Michigan 48109, United States;* orcid.org/0000-0002-8149-5417; Email: brookscl@umich.edu

Anna K. Mapp − *Life Sciences Institute, University of Michigan, Ann Arbor, Michigan 48019, United States; Program in Chemical Biology and Department of Chemistry, University of Michigan, Ann Arbor, Michigan 48109, United States;* orcid.org/0000-0003-0791-8327; Email: amapp@umich.edu

Authors

Amanda L. Peiffer − *Life Sciences Institute, University of Michigan, Ann Arbor, Michigan 48019, United States; Program in Chemical Biology, University of Michigan, Ann Arbor, Michigan 48109, United States*

Julie M. Garlick − *Life Sciences Institute, University of Michigan, Ann Arbor, Michigan 48019, United States; Department of Chemistry, University of Michigan, Ann Arbor, Michigan 48109, United States*

Yujin Wu − *Department of Chemistry, University of Michigan, Ann Arbor, Michigan 48109, United States*

Jesse W. Wotring − *Department of Medicinal Chemistry, College of Pharmacy, University of Michigan, Ann Arbor, Michigan 48109, United States*

Sahil Arora − *Department of Chemistry, University of Michigan, Ann Arbor, Michigan 48109, United States*

Alexander S. Harmata − *Department of Chemistry, University of Michigan, Ann Arbor, Michigan 48109, United States*

Daniel A. Bochar − *Department of Chemistry, University of Michigan, Ann Arbor, Michigan 48109, United States*

Corey J. Stephenson − *Department of Chemistry, University of Michigan, Ann Arbor, Michigan 48109, United States;* orcid.org/0000-0002-2443-5514

Matthew B. Soellner − *Program in Chemical Biology and Department of Chemistry, University of Michigan, Ann Arbor, Michigan 48109, United States;* orcid.org/0000-0003-1394-8645

Jonathan Z. Sexton − *Department of Medicinal Chemistry, College of Pharmacy, University of Michigan, Ann Arbor, Michigan 48109, United States; University of Michigan Medical School, Ann Arbor, Michigan 48109, United States*

Complete contact information is available at: https://pubs.acs.org/10.1021/acsmedchemlett.3c00035

Author Contributions

¶These authors contributed equally.

Notes

The authors declare no competing financial interest.

■ ACKNOWLEDGMENTS

We acknowledge the valuable scientific input of Dr. Kevon Stanford, Tessa Epstein, Ayza Croskey, Dr. Stephen Joy, Furyal Ahmed, Dr. Allison Narayan, and Dr. Madison Sowden. Research reported in this publication was supported by the Center for Chemical Genomics (CCG) at the University of Michigan Life Sciences Institute. Financial support for this

https://doi.org/10.1021/acsmedchemlett.3c00035
ACS Med. Chem. Lett. 2023, 14, 860−866

work was provided by the Klatskin-Sutker Discovery Fund award (to A.K.M.) and the National Institutes of Health Grants GM103695 (to C.L.B), GM130587 (to C.L.B), and GM136356 (to A.K.M.).

REFERENCES

(1) Cully, M. A tale of two antiviral targets - and the COVID-19 drugs that bind them. *Nat. Rev. Drug Discovery* **2022**, *21* (1), 3−5.
(2) Hoffmann, M.; Kleine-Weber, H.; Schroeder, S.; Kruger, N.; Herrler, T.; Erichsen, S.; Schiergens, T. S.; Herrler, G.; Wu, N. H.; Nitsche, A.; Muller, M. A.; Drosten, C.; Pohlmann, S. SARS-CoV-2 Cell Entry Depends on ACE2 and TMPRSS2 and Is Blocked by a Clinically Proven Protease Inhibitor. *Cell.* **2020**, *181* (2), 271−80.
(3) V'Kovski, P.; Kratzel, A.; Steiner, S.; Stalder, H.; Thiel, V. Coronavirus biology and replication: implications for SARS-CoV-2. *Nat. Rev. Microbiol.* **2021**, *19* (3), 155−70.
(4) Kim, T. S.; Heinlein, C.; Hackman, R. C.; Nelson, P. S. Phenotypic analysis of mice lacking the Tmprss2-encoded protease. *Mol. Cell. Biol.* **2006**, *26* (3), 965−75.
(5) Stopsack, K. H.; Mucci, L. A.; Antonarakis, E. S.; Nelson, P. S.; Kantoff, P. W. TMPRSS2 and COVID-19: Serendipity or Opportunity for Intervention? *Cancer Discovery* **2020**, *10* (6), 779−82.
(6) Shulla, A.; Heald-Sargent, T.; Subramanya, G.; Zhao, J.; Perlman, S.; Gallagher, T. A transmembrane serine protease is linked to the severe acute respiratory syndrome coronavirus receptor and activates virus entry. *J. Virol.* **2011**, *85* (2), 873−82.
(7) Matsuyama, S.; Nagata, N.; Shirato, K.; Kawase, M.; Takeda, M.; Taguchi, F. Efficient activation of the severe acute respiratory syndrome coronavirus spike protein by the transmembrane protease TMPRSS2. *J. Virol.* **2010**, *84* (24), 12658−64.
(8) Shirato, K.; Kawase, M.; Matsuyama, S. Middle East respiratory syndrome coronavirus infection mediated by the transmembrane serine protease TMPRSS2. *J. Virol.* **2013**, *87* (23), 12552−61.
(9) Shen, L. W.; Mao, H. J.; Wu, Y. L.; Tanaka, Y.; Zhang, W. TMPRSS2: A potential target for treatment of influenza virus and coronavirus infections. *Biochimie.* **2017**, *142*, 1−10.
(10) Rosendal, E.; Mihai, I. S.; Becker, M.; Das, D.; Frängsmyr, L.; Persson, B. D.; Rankin, G. D.; Gröning, R.; Trygg, J.; Forsell, M.; Ankarklev, J.; Blomberg, A.; Henriksson, J.; Överby, A. K.; Lenman, A. Serine Protease Inhibitors Restrict Host Susceptibility to SARS-CoV-2 Infections. *mBio.* **2022**, *13*, No. e0089222.
(11) Hatesuer, B.; Bertram, S.; Mehnert, N.; Bahgat, M. M.; Nelson, P. S.; Pohlman, S.; Schughart, K. Tmprss2 is essential for influenza H1N1 virus pathogenesis in mice. *PLoS Pathog.* **2013**, *9* (12), No. e1003774.
(12) Qiao, Y.; Wang, X. M.; Mannan, R.; Pitchiaya, S.; Zhang, Y.; Wotring, J. W.; Xiao, L.; Robinson, D. R.; Wu, Y. M.; Tien, J. C.; Cao, X.; Simko, S. A.; Apel, I. J.; Bawa, P.; Kregel, S.; Narayanan, S. P.; Raskind, G.; Ellison, S. J.; Parolia, A.; Zelenka-Wang, S.; McMurry, L.; Su, F.; Wang, R.; Cheng, Y.; Delekta, A. D.; Mei, Z.; Pretto, C. D.; Wang, S.; Mehra, R.; Sexton, J. Z.; Chinnaiyan, A. M. Targeting transcriptional regulation of SARS-CoV-2 entry factors ACE2 and TMPRSS2. *Proc. Natl. Acad. Sci. U. S. A.* **2021**, *118* (1), e2021450118.
(13) Mahoney, M.; Damalanka, V. C.; Tartell, M. A.; Chung, D. H.; Lourenco, A. L.; Pwee, D.; Mayer Bridwell, A. E.; Hoffmann, M.; Voss, J.; Karmakar, P.; Azouz, N. P.; Klingler, A. M.; Rothlauf, P. W.; Thompson, C. E.; Lee, M.; Klampfer, L.; Stallings, C. L.; Rothenberg, M. E.; Pohlmann, S.; Whelan, S. P. J.; O'Donoghue, A. J.; Craik, C. S.; Janetka, J. W. A novel class of TMPRSS2 inhibitors potently block SARS-CoV-2 and MERS-CoV viral entry and protect human epithelial lung cells. *Proc. Natl. Acad. Sci. U. S. A.* **2021**, *118* (43), e2108728118.
(14) Shapira, T.; Monreal, I. A.; Dion, S. P.; Buchholz, D. W.; Imbiakha, B.; Olmstead, A. D.; Jager, M.; Désilets, A.; Gao, G.; Martins, M.; Vandal, T.; Thompson, C. A. H.; Chin, A.; Rees, W. D.; Steiner, T.; Nabi, I. R.; Marsault, E.; Sahler, J.; Diel, D. G.; Van de Walle, G. R.; August, A.; Whittaker, G. R.; Boudreault, P. L.; Leduc, R.; Aguilar, H. C.; Jean, F. A TMPRSS2 inhibitor acts as a pan-SARS-CoV-2 prophylactic and therapeutic. *Nature.* **2022**, *605* (7909), 340−8.
(15) Mantzourani, C.; Vasilakaki, S.; Gerogianni, V. E.; Kokotos, G. The discovery and development of transmembrane serine protease 2 (TMPRSS2) inhibitors as candidate drugs for the treatment of COVID-19. *Expert Opin Drug Discovery* **2022**, *17* (3), 231−46.
(16) Hu, X.; Shrimp, J. H.; Guo, H.; Xu, M.; Chen, C. Z.; Zhu, W.; Zakharov, A. V.; Jain, S.; Shinn, P.; Simeonov, A.; Hall, M. D.; Shen, M. Discovery of TMPRSS2 Inhibitors from Virtual Screening as a Potential Treatment of COVID-19. *ACS Pharmacol Transl Sci.* **2021**, *4* (3), 1124−35.
(17) Breining, P.; Frolund, A. L.; Hojen, J. F.; Gunst, J. D.; Staerke, N. B.; Saedder, E.; Cases-Thomas, M.; Little, P.; Nielsen, L. P.; Sogaard, O. S.; Kjolby, M. Camostat mesylate against SARS-CoV-2 and COVID-19-Rationale, dosing and safety. *Basic Clin Pharmacol Toxicol.* **2021**, *128* (2), 204−12.
(18) Shrimp, J. H.; Kales, S. C.; Sanderson, P. E.; Simeonov, A.; Shen, M.; Hall, M. D. An Enzymatic TMPRSS2 Assay for Assessment of Clinical Candidates and Discovery of Inhibitors as Potential Treatment of COVID-19. *ACS Pharmacol Transl Sci.* **2020**, *3* (5), 997−1007.
(19) Hofmann-Winkler, H.; Moerer, O.; Alt-Epping, S.; Brauer, A.; Buttner, B.; Muller, M.; Fricke, T.; Grundmann, J.; Harnisch, L. O.; Heise, D.; Kernchen, A.; Pressler, M.; Stephani, C.; Tampe, B.; Kaul, A.; Gartner, S.; Kramer, S.; Pohlmann, S.; Winkler, M. S. Camostat Mesylate May Reduce Severity of Coronavirus Disease 2019 Sepsis: A First Observation. *Crit Care Explor.* **2020**, *2* (11), No. e0284.
(20) Wang, D.; Li, Z.; Liu, Y. An overview of the safety, clinical application and antiviral research of the COVID-19 therapeutics. *J. Infect Public Health.* **2020**, *13* (10), 1405−14.
(21) Spraggon, G.; Hornsby, M.; Shipway, A.; Tully, D. C.; Bursulaya, B.; Danahay, H.; Harris, J. L.; Lesley, S. A. Active site conformational changes of prostasin provide a new mechanism of protease regulation by divalent cations. *Protein Sci.* **2009**, *18* (5), 1081−94.
(22) Sun, W.; Zhang, X.; Cummings, M. D.; Albarazanji, K.; Wu, J.; Wang, M.; Alexander, R.; Zhu, B.; Zhang, Y.; Leonard, J.; Lanter, J.; Lenhard, J. Targeting Enteropeptidase with Reversible Covalent Inhibitors To Achieve Metabolic Benefits. *J. Pharmacol Exp Ther.* **2020**, *375* (3), 510−21.
(23) Hempel, T.; Raich, L.; Olsson, S.; Azouz, N. P.; Klingler, A. M.; Hoffmann, M.; Pohlmann, S.; Rothenberg, M. E.; Noe, F. Molecular mechanism of inhibiting the SARS-CoV-2 cell entry facilitator TMPRSS2 with camostat and nafamostat. *Chem. Sci.* **2021**, *12* (3), 983−92.
(24) Paoloni-Giacobino, A.; Chen, H.; Peitsch, M. C.; Rossier, C.; Antonarakis, S. E. Cloning of the TMPRSS2 gene, which encodes a novel serine protease with transmembrane, LDLRA, and SRCR domains and maps to 21q22.3. *Genomics.* **1997**, *44* (3), 309−20.
(25) Xia, X. Domains and Functions of Spike Protein in Sars-Cov-2 in the Context of Vaccine Design. *Viruses* **2021**, *13* (1), 109.
(26) Afar, D. E.; Vivanco, I.; Hubert, R. S.; Kuo, J.; Chen, E.; Saffran, D. C.; Raitano, A. B.; Jakobovits, A. Catalytic cleavage of the androgen-regulated TMPRSS2 protease results in its secretion by prostate and prostate cancer epithelia. *Cancer Res.* **2001**, *61* (4), 1686−1692.
(27) Waterhouse, A.; Bertoni, M.; Bienert, S.; Studer, G.; Tauriello, G.; Gumienny, R.; Heer, F. T.; de Beer, T. A. P.; Rempfer, C.; Bordoli, L.; Lepore, R.; Schwede, T. SWISS-MODEL: homology modelling of protein structures and complexes. *Nucleic Acids Res.* **2018**, *46* (W1), W296−W303.
(28) Fraser, B. J.; Beldar, S.; Seitova, A.; Hutchinson, A.; Mannar, D.; Li, Y.; Kwon, D.; Tan, R.; Wilson, R. P.; Leopold, K.; Subramaniam, S.; Halabelian, L.; Arrowsmith, C. H.; Bénard, F. Structure, activity and inhibition of human TMPRSS2, a protease implicated in SARS-CoV-2 activation. *Nat. Chem. Biol.* **2022**, *18*, 963−971.

https://doi.org/10.1021/acsmedchemlett.3c00035
ACS Med. Chem. Lett. 2023, 14, 860−866

(29) Ding, X.; Wu, Y.; Wang, Y.; Vilseck, J. Z.; Brooks, C. L., 3rd Accelerated CDOCKER with GPUs, Parallel Simulated Annealing, and Fast Fourier Transforms. *J. Chem. Theory Comput.* **2020**, *16* (6), 3910−9.
(30) Wu, G.; Robertson, D. H.; Brooks, C. L., 3rd; Vieth, M. Detailed analysis of grid-based molecular docking: A case study of CDOCKER-A CHARMm-based MD docking algorithm. *J. Comput. Chem.* **2003**, *24* (13), 1549−62.
(31) Brooks, B. R.; Brooks, C. L., 3rd; Mackerell, A. D., Jr; Nilsson, L.; Petrella, R. J.; Roux, B.; Won, Y.; Archontis, G.; Bartels, C.; Boresch, S.; Caflisch, A.; Caves, L.; Cui, Q.; Dinner, A. R.; Feig, M.; Fischer, S.; Gao, J.; Hodoscek, M.; Im, W.; Kuczera, K.; Lazaridis, T.; Ma, J.; Ovchinnikov, V.; Paci, E.; Pastor, R. W.; Post, C. B.; Pu, J. Z.; Schaefer, M.; Tidor, B.; Venable, R. M.; Woodcock, H. L.; Wu, X.; Yang, W.; York, D. M.; Karplus, M. CHARMM: the biomolecular simulation program. *J. Comput. Chem.* **2009**, *30* (10), 1545−614.
(32) Stone, A. J.; Erskine, R. W. INTERMOLECULAR SELF-CONSISTENT-FIELD PERTURBATION-THEORY FOR ORGANIC-REACTIONS.1. THEORY AND IMPLEMENTATION - NUCLEOPHILIC-ATTACK ON CARBONYL-COMPOUNDS. *J. Am. Chem. Soc.* **1980**, *102* (24), 7185−92.
(33) Fox, J. M.; Dmitrenko, O.; Liao, L. A.; Bach, R. D. Computational studies of nucleophilic substitution at carbonyl carbon: the S(N)2 mechanism versus the tetrahedral intermediate in organic synthesis. *J. Org. Chem.* **2004**, *69* (21), 7317−7328.
(34) Scheiner, S.; Lipscomb, W. N.; Kleier, D. A. Molecular orbital studies of enzyme activity. 2. Nucleophilic attack on carbonyl systems with comments on orbital steering. *J. Am. Chem. Soc.* **1976**, *98* (16), 4770−7.
(35) Lucas, J. M.; Heinlein, C.; Kim, T.; Hernandez, S. A.; Malik, M. S.; True, L. D.; Morrissey, C.; Corey, E.; Montgomery, B.; Mostaghel, E.; Clegg, N.; Coleman, I.; Brown, C. M.; Schneider, E. L.; Craik, C.; Simon, J. A.; Bedalov, A.; Nelson, P. S. The androgen-regulated protease TMPRSS2 activates a proteolytic cascade involving components of the tumor microenvironment and promotes prostate cancer metastasis. *Cancer Discovery* **2014**, *4* (11), 1310−25.
(36) Koch, J.; Uckeley, Z. M.; Doldan, P.; Stanifer, M.; Boulant, S.; Lozach, P. Y. TMPRSS2 expression dictates the entry route used by SARS-CoV-2 to infect host cells. *EMBO J.* **2021**, *40* (16), No. e107821.
(37) Peacock, T. P.; Goldhill, D. H.; Zhou, J.; Baillon, L.; Frise, R.; Swann, O. C.; Kugathasan, R.; Penn, R.; Brown, J. C.; Sanchez-David, R. Y.; Braga, L.; Williamson, M. K.; Hassard, J. A.; Staller, E.; Hanley, B.; Osborn, M.; Giacca, M.; Davidson, A. D.; Matthews, D. A.; Barclay, W. S. The furin cleavage site in the SARS-CoV-2 spike protein is required for transmission in ferrets. *Nat. Microbiol.* **2021**, *6* (7), 899−909.
(38) Chen, R. E.; Zhang, X.; Case, J. B.; Winkler, E. S.; Liu, Y.; VanBlargan, L. A.; Liu, J.; Errico, J. M.; Xie, X.; Suryadevara, N.; Gilchuk, P.; Zost, S. J.; Tahan, S.; Droit, L.; Turner, J. S.; Kim, W.; Schmitz, A. J.; Thapa, M.; Wang, D.; Boon, A. C. M.; Presti, R. M.; O'Halloran, J. A.; Kim, A. H. J.; Deepak, P.; Pinto, D.; Fremont, D. H.; Crowe, J. E., Jr; Corti, D.; Virgin, H. W.; Ellebedy, A. H.; Shi, P. Y.; Diamond, M. S. Resistance of SARS-CoV-2 variants to neutralization by monoclonal and serum-derived polyclonal antibodies. *Nat. Med.* **2021**, *27* (4), 717−26.
(39) Garcia-Beltran, W. F.; Lam, E. C.; St Denis, K.; Nitido, A. D.; Garcia, Z. H.; Hauser, B. M.; Feldman, J.; Pavlovic, M. N.; Gregory, D. J.; Poznansky, M. C.; Sigal, A.; Schmidt, A. G.; Iafrate, A. J.; Naranbhai, V.; Balazs, A. B. Multiple SARS-CoV-2 variants escape neutralization by vaccine-induced humoral immunity. *Cell.* **2021**, *184* (9), 2523.

https://doi.org/10.1021/acsmedchemlett.3c00035
ACS Med. Chem. Lett. 2023, 14, 860−866